

## Two-Photon Spectroscopy of the Acetaldehyde–Ar Complex

Y. Kim, J. Fleniken, and H. Meyer\*

Department of Physics and Astronomy, The University of Georgia, Athens, Georgia 30602-2451

Received: February 22, 1999; In Final Form: June 28, 1999

The two-photon spectrum of the acetaldehyde–Ar complex has been measured in the vicinity of the (n,3s) Rydberg transition of the acetaldehyde monomer. The cluster spectrum is blue shifted by  $14\text{ cm}^{-1}$  from the monomer origin. The vibrational analysis yields harmonic frequencies of 32, 27, and  $21\text{ cm}^{-1}$  for the intermolecular modes. The two high-frequency modes are Franck–Condon active, indicating a substantial displacement of the minimum configuration with respect to the ground-state equilibrium structure. The abrupt disappearance of the vibrational structure at energies of about  $190\text{ cm}^{-1}$  above the origin is interpreted as the dissociation limit of the complex.

### 1. Introduction

Over the past two decades, van der Waals complexes have been the focus of intense research, both experimentally and theoretically.<sup>1</sup> Especially, small hydrogen bonded complexes have been studied intensely in the microwave, far-infrared, and infrared regions of the electromagnetic spectrum.<sup>2</sup> Electronic spectroscopy of molecular complexes has been limited almost exclusively to complexes containing atoms, molecules, or radicals with low-lying electronic states. On the other hand, the first excited states of a number of small molecules lie in the vacuum ultraviolet (VUV) spectral region and are therefore not easily accessible using conventional laser sources. For some of these molecules, nonresonant two-photon absorption has been shown to be a suitable alternative to access transitions in the VUV. Beside the spectroscopic interest, two-photon transitions of several molecular species are sufficiently strong to be employed for the state-specific product detection in molecular dynamics studies.<sup>3–9</sup> Another interesting candidate is acetaldehyde and its two-photon transition to the (n,3s) Rydberg state.<sup>10–13</sup> This two-photon transition is exceptionally strong due to a near resonance of the first excited-state  $S_1$  with the virtual intermediate state. Recently, we were able to analyze the rotational structure of several observed bands including the torsional sequence.<sup>14,15</sup>

As a stable intermediate in the oxidation of hydrocarbons, acetaldehyde represents an important air pollutant.<sup>16</sup> Subsequent reactions with both the hydroxyl radical and the nitrate radical result in the formation of peroxyacetyl nitrate, an important reservoir species for reactive nitrogen. UV photodissociation of acetaldehyde has been identified as the other major loss mechanism. Therefore, there is a great interest in understanding the spectroscopy, photophysics, and photochemistry of acetaldehyde and its complexes. Although the acetaldehyde molecule is a relatively small molecule with the same mass as the  $\text{CO}_2$  molecule, it has several particular features which will influence its dynamics. Not only is it an asymmetric top molecule of low symmetry it also has two distinct functional groups: a carbonyl group and a methyl internal rotor. Thus, acetaldehyde can serve as a prototype to study the influence of these functional groups on molecular interactions and reactivities.

Of special interest will be the effect of the internal rotor on the inter- and/or intramolecular vibrational relaxation (IVR) dynamics. Similar to an open-shell molecule, acetaldehyde has an internal angular momentum, although it originates from a very different source. Similarities and differences in the collision and predissociation dynamics in comparison with the dynamics of an open-shell complex need to be explored. In large aromatic molecules, the presence of an internal rotor enhances the IVR rate substantially.<sup>17–19</sup> These findings are usually explained in terms of the strongly increased density of states and the coupling of vibrational and torsional modes mediated through repulsive van der Waals interactions.<sup>20–22</sup> In the case of a high barrier to internal rotation, Tan et al. suggest the coupling of internal and overall rotation as a possible additional source for level interactions.<sup>23</sup> These authors noticed a strong correlation of the strength of these interactions with the direction of the rotor axis. Unfortunately, there are no detailed studies of how the methyl group affects rovibrational energy transfer in bimolecular collisions. The possibility of state-specific detection of acetaldehyde via two-photon absorption offers new possibilities to study these effects in unprecedented detail. In a counterpropagating molecular beam scattering experiment, we investigated the energy transfer of acetaldehyde in collisions with different rare gas partners. In these experiments, we observe efficient excitation of the torsional levels below the barrier to internal rotation. The preliminary analysis suggests as the dominant excitation mechanism the strong coupling of the torsional motion with the overall rotation.<sup>24</sup>

As another means of studying the molecular interactions responsible for rovibrational energy transfer, the corresponding van der Waals complex can be investigated spectroscopically. A great variety of complexes have been studied using either optothermal or direct absorption techniques.<sup>25,26</sup> In a small number of experiments, double resonance schemes have been applied.<sup>27,28</sup> While it is possible to cover a wide range of frequencies with the employed pulsed lasers, the spectral resolution is usually limited to a few tenths of a wavenumber. Exploiting one-photon resonances, both UV-detected stimulated Raman as well as infrared absorption of clusters have been reported.<sup>29–33</sup> In refs 34 and 35, two-photon resonances have been used for the fragment detection step. Direct detection of an unfragmented complex through nonresonant two-photon

\* Corresponding author. E-mail: hmeyer@hal.physast.uga.edu.

absorption could allow one to access higher lying excited electronic states and therefore to investigate complexes involving smaller molecules. So far, only complexes involving atoms or diatomic molecules have been detected through nonresonant two-photon absorption. In particular, van der Waals complexes involving either NO, HI, or Xe as the two-photon chromophore have been reported.<sup>36–39</sup> To analyze these spectra, we extended the spherical tensor treatment of the two-photon absorption operator to the case of a rigid rotor type van der Waals complex in which the excitation is confined to the two-photon chromophore.<sup>40,41</sup> In this way, we were able to analyze the partially resolved rotational structure in the two-photon spectra observed for several NO-containing complexes.<sup>41–43</sup>

Recently, the microwave spectrum of the acetaldehyde–Ar complex has been reported by Ioannou et al.<sup>44</sup> From this study, a structure was derived which places the Ar atom on top of the triangle formed by the heavy atoms of the acetaldehyde molecule. Assuming a Lennard-Jones potential, the authors were able to derive from the centrifugal distortion constants a binding energy of about 204  $\text{cm}^{-1}$ . Furthermore, the splitting of the rotational lines into quartets has been interpreted in terms of two tunneling paths involving internal rotation of the methyl group as well as the internal rotation of the acetaldehyde unit within the complex.<sup>45</sup> Unfortunately, the observed splittings did not allow the determination of a barrier height for either tunneling pathway. It is interesting to note that electronic spectra (B–X transition) have been reported also for the related complexes HCO–Ar and  $\text{CH}_2\text{CHO}$ –Ar.<sup>46,47</sup> In both cases, the Ar atom is found to interact dominantly with the CO group causing an increase of the binding energy for the excited state. In the case of the Ar–vinoxy complex, an out-of-plane structure could be deduced from the rotational contour analysis. The observed red shift is explained in terms of a lowering of the in-plane barrier to internal rotation.

In this contribution, we report the first two-photon spectrum of a van der Waals complex involving the polyatomic molecule acetaldehyde. The purpose of this study is two-fold. First, we want to explore the structure of the excited-state potential energy surface. Second, the ability of detecting unfragmented molecular complexes through (2 + 1) REMPI opens new possibilities for studying bound states of the electronic ground-state surface through infrared–ultraviolet double resonance experiments.

## 2. Experimental Section

The experiment was performed using a pulsed molecular beam scattering apparatus which has been described in detail previously.<sup>4,5</sup> Briefly, a gas mixture of 4% acetaldehyde in Ar was expanded into vacuum at a stagnation pressure of 1.5 bar using a home-built piezoelectric valve. Molecular beam pulses of about 75  $\mu\text{s}$  duration were generated at a repetition rate of 10 Hz. The pulses passed through a skimmer into the detection chamber where they were intersected with a laser beam. Ions resulting from the (2 + 1) REMPI process were mass and velocity selected in a time-of-flight (TOF) mass spectrometer. The laser system employed was a Nd:YAG pumped near-grazing incidence dye laser operating on the laser dye Pyridine 2. The dye laser output was frequency doubled in a KDP crystal and focused onto the molecular beam using a lens of 300 mm focal length. Pulse energies of about 1 mJ were employed for the detection of the cluster spectrum.

Typical TOF spectra are shown in Figure 1. The spectrum in the upper part shows the mass spectrum obtained by exciting the acetaldehyde monomer in the  $10^1_0$  band of the (n,3s) Rydberg transition using pulse energies of about 250  $\mu\text{J}$ . Under

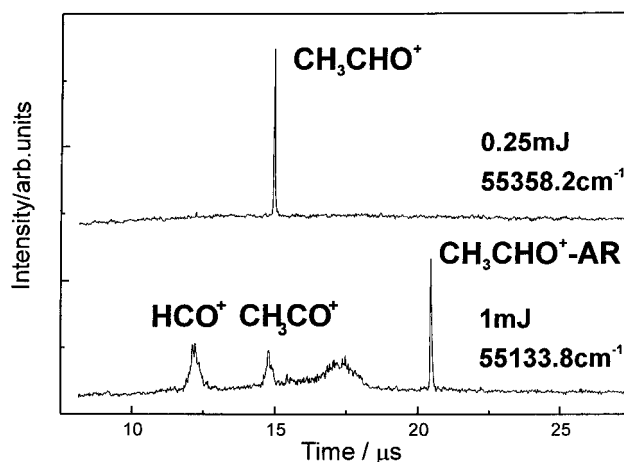


**Figure 1.** Time-of-flight mass spectra recorded at the specified two-photon wavenumbers. Both spectra were recorded under identical ion imaging conditions. The peak in the upper spectrum represents acetaldehyde ions (44 amu). At this frequency the  $10^1_0$  mode of the (n,3s) Rydberg transition is excited. The bottom spectrum was recorded with the laser tuned to a frequency at which a cluster band is excited. Both unfragmented acetaldehyde–Ar ions and ionized fragments were detected.

these conditions, no fragmentation of the acetaldehyde molecule is observed. The bottom spectrum is recorded with the laser frequency tuned to 27 567  $\text{cm}^{-1}$ , corresponding to a two-photon wavenumber of 55 134  $\text{cm}^{-1}$ . At this frequency, a peak is detected at a flight time of about 21  $\mu\text{s}$ , which corresponds to an ion mass of 84 amu. Like the peak due to the acetaldehyde monomer in the upper spectrum, the width of this peak is limited by the instrumental resolution. In contrast, we observe significantly broader peaks at flight times corresponding to ion masses of 29 amu ( $\text{HCO}^+$ ) and 43 amu ( $\text{CH}_3\text{CO}^+$ ). These ions result from the excitation, ionization, and fragmentation of acetaldehyde molecules and possible larger clusters in the beam. The width of the peaks reflects the energy release as a consequence of the fragmentation process. The peak centered at 17.5  $\mu\text{s}$  is due to electron impact ionization of Ar from the molecular beam. The responsible electrons are most likely created as photoelectrons due to the interaction of stray laser light with the various metal electrodes, etc. Therefore, the location for ionization is not well defined, resulting in a broad distribution of flight times which are longer than what would be expected for a direct laser ionization process. Since the 84 amu peak is characterized by a width typical for unfragmented species, we identify this peak as resulting from the resonant excitation of the neutral acetaldehyde–Ar complex. The possibility of the signal resulting from the acetaldehyde dimer (88 amu) is ruled out by the fact that the cluster bands are absent if acetaldehyde is used with neon as the carrier gas. REMPI spectra were measured by recording the intensity of this mass peak as a function of the laser frequency.

For the case that the employed UV photons are not sufficient to ionize the complex under investigation, we used a two-color REMPI detection scheme. The doubled outputs of two dye lasers, L1 and L2, were focused with 300 mm lenses onto the molecular beam, resulting in spots of about 30  $\mu\text{m}$  in diameter. Both laser beams were counterpropagating and intersected the molecular beam at right angles. The frequency of the ionization laser L2 was tuned to 29 656  $\text{cm}^{-1}$ . In this frequency range, acetaldehyde can be detected through a (1 + 2) REMPI process with the first excited-state  $S_1$  acting as the intermediate state.<sup>11</sup> For the two-color experiment, the wavelength of the ionization laser was carefully chosen in a way not to produce a one-color

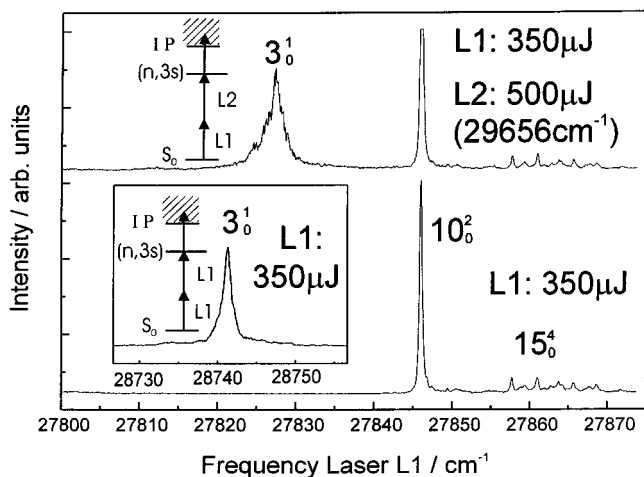


**Figure 2.** Nonresonant two-color ( $1 + 1' + 1$ ) REMPI spectrum of the acetaldehyde monomer. The frequency of laser L2 was fixed to  $29\,656\text{ cm}^{-1}$ , while the frequency of laser L1 was tuned. The top spectrum shows the two-color resonance due to the excitation of the  $3^1_0$  mode in acetaldehyde. The bottom spectrum was recorded without laser L2. The inset displays the one-color ( $2 + 1$ ) REMPI spectrum of the  $3^1_0$  band. See text for details.

ionization signal. To verify the alignment of the two focused laser beams, we searched for double resonance signals in the acetaldehyde monomer spectrum. As a convenient band in the available wavelength range, we detected the band  $3^1_0$ .<sup>48</sup> The one-color resonance was found with the laser frequency tuned to  $28\,741.5\text{ cm}^{-1}$  corresponding to a two-photon wavenumber of  $57\,483\text{ cm}^{-1}$ . In the two-color experiment, resonant excitation requires the simultaneous absorption of a photon from both lasers:  $57\,483\text{ cm}^{-1} = 27\,827\text{ cm}^{-1}$  (L1) +  $29\,656\text{ cm}^{-1}$  (L2). This band provides a straightforward verification of the spatial and temporal overlap of the laser beams.

A typical two-color ( $1 + 1' + 1$ ) REMPI spectrum is displayed in Figure 2. The top part shows the spectrum recorded with both laser beams present, while the bottom part was recorded without laser L2. In this range, several weak monomer bands were also observed as one-color ( $2 + 1$ ) REMPI signals. In particular, the bands  $10^2_0$  and several rotational lines of the band  $15^4_0$  were found. The inset in Figure 2 displays the one-color spectrum of the  $3^1_0$  band using the same frequency and intensity scale. In comparison with the other monomer bands, we find the width of the  $3^1_0$  band to be increased significantly. This is especially true for the two-color spectrum. This increase in line width as well as the asymmetric line shape for the two-color result is most likely caused by the near resonance of the frequency of the ionization laser L2 with the origin of the  $S_1 - S_0$  transition at  $29\,771\text{ cm}^{-1}$ .<sup>49</sup> Most important for this study is the fact that the two-color spectrum is comparable in intensity to the corresponding one-color REMPI spectrum. Thus, the two-color experiment provides us with a sensitivity comparable to the one achieved in the single-color experiment.

### 3. Results and Interpretation

An overview ( $2 + 1$ ) REMPI spectrum of the region of the  $0^0_0$  and  $10^1_0$  bands of the ( $n,3s$ ) Rydberg transition in acetaldehyde is shown in Figure 3. The bottom spectrum was measured recording the mass peak corresponding to the acetaldehyde ion mass (44 amu). The origin band was found at a two-photon energy of  $55\,024.5\text{ cm}^{-1}$ . The peak at  $55\,358.2\text{ cm}^{-1}$  is assigned to the excitation of the  $10^1_0$  mode which involves mainly the C–C–O bending vibration. The weak band at  $55\,426\text{ cm}^{-1}$  is assigned to the excitation of the torsional band  $15^2_0$

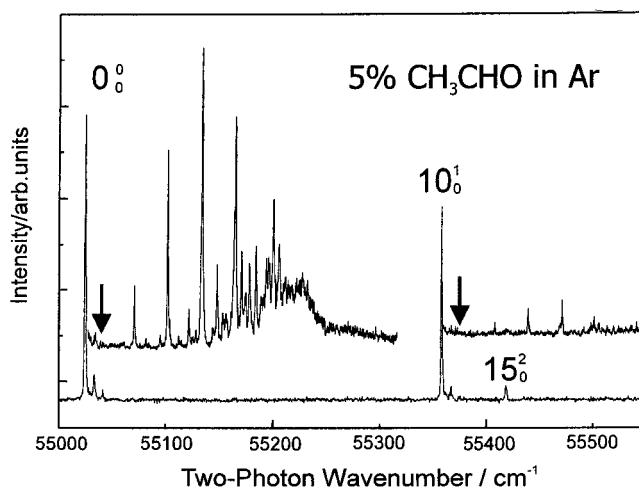


**Figure 3.** Overview ( $2 + 1$ ) REMPI spectra recorded at the acetaldehyde monomer mass (44 amu) and the mass of its complex with Ar (84 amu). The cluster spectra were recorded with a laser pulse energy of about 1 mJ and the ion detector at full sensitivity.

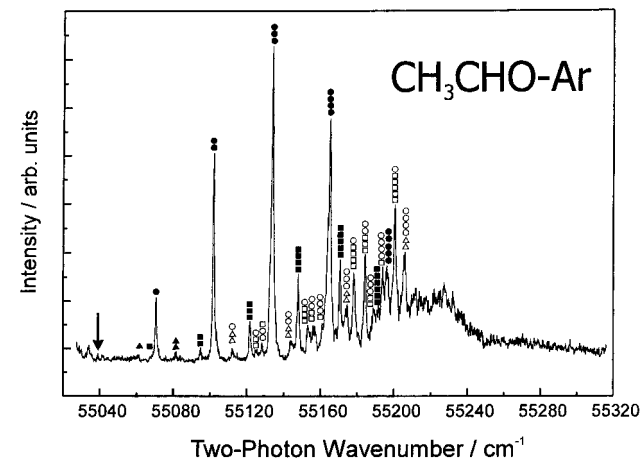


**Figure 4.** Expanded ( $2 + 1$ ) REMPI spectrum of the acetaldehyde–Ar complex. The arrow indicates the possible position of the origin for this band system. Vibrational bands are marked with the number of vibrational quanta involved. See text for details.

characterized by a very small Franck–Condon factor. Each torsionless band is accompanied to the blue by a series of weak satellite bands, which have been identified as rotational structure.<sup>14</sup> The analysis of these features indicates a rotational temperature of about 4 K. From the thermal rest population of different torsional levels, a torsional temperature of about 25 K can be estimated. Since complexes are preferentially formed from cold parent molecules, an even lower temperature is expected for the acetaldehyde–Ar complex.

The spectra in the top part of Figure 3 were recorded at mass 84 amu and assigned to the acetaldehyde–Ar complex. The spectrum is made up of two contributions. One is located between the monomer origin band and the monomer  $10^1_0$  mode, and the other is located to the blue of the  $10^1_0$  mode. The intensity of the latter spectrum is reduced by more than order of magnitude. Using either one-color or two-color REMPI detection, no cluster signal could be detected to the red of the origin band. Since all frequencies were determined as one-color REMPI signals, we report in the following the two-photon wavenumbers only.

Figure 4 shows an expanded view of the acetaldehyde–Ar spectrum located to the blue of the monomer origin band. At the low-frequency end of the spectrum, a series of well-resolved

**TABLE 1: Two-Photon Wavenumbers  $\nu$  and Relative Franck–Condon Factors  $x_{fc}$  of the Observed Vibronic Bands of the Acetaldehyde–Ar Complex in an Electronic State Correlating with the Origin of the (n,3s) Rydberg State**

mode	$\nu_c, \nu_s, \nu_t$	$\nu^a$ (cm <sup>-1</sup> )	$\Delta\nu^a$ (cm <sup>-1</sup> )	$x_{fc}$
triangle	0,0,0	55038.6	22.5	<0.5
	0,0,1	55061.0	20.7	1.0
	0,0,2	55081.7		3.0
square	0,0,0	55038.6	28.8	<0.5
	0,1,0	55067.4	27.3	1.5
	0,2,0	55094.7	26.9	4.0
	0,3,0	55121.6	26.3	15.0
	0,4,0	55147.9	22.8	34.0
	0,5,0	55170.7		40.0
	circle	0,0,0	55038.6	32.1
1,0,0		55070.7	31.1	25.0
2,0,0		55101.8	32.0	82.5
3,0,0		55133.8	31.3	124.5
4,0,0		55165.1	31.0	95.0
5,0,0		55196.1		37.0
0,0,2		55081.7	30.2	3.0
1,0,2		55111.9	31.6	4.5
2,0,2		55143.5	31.0	8.0
3,0,2		55174.5	31.4	22.0
4,0,2		55205.9		43.0
1,0,0		55070.7		25.0
1,1,0			54.9	
1,2,0		55125.6	27.5	3.5
1,3,0		55153.1	24.9	14.0
1,4,0		55178.0	21.9	35.0
1,5,0		55199.9		61.0
2,0,0		55101.8	26.3	82.5
2,1,0		55128.1	28.2	7.5
2,2,0		55156.3	28.0	14.0
2,3,0	55184.3		42.0	

<sup>a</sup> Frequency intervals  $\Delta\nu$  between different members of the assigned progressions.

bands is observed. A summary of the band positions, their relative spacings, and assignments is given in Table 1. With increasing energy, the number of lines increases steadily until an almost continuous signal is observed for frequencies larger than 55 210 cm<sup>-1</sup>. The pronounced intensity drop at 55 240 cm<sup>-1</sup> is reminiscent of a threshold, although the intensity does not completely drop to zero. At a frequency of 55 300 cm<sup>-1</sup>, we are still able to detect a small but noticeable signal. At these frequencies, the time-of-flight spectra are consistent with the detection of long-lived, unfragmented complexes.

The weak band system observed to the blue of the monomer band 10<sup>1</sup><sub>0</sub> is assigned to the corresponding band of the acetaldehyde–Ar complex. An expanded view is shown in Figure 5. The bands in this system show a spacing and intensity distribution very similar to the ones in the strong system to the blue of the origin band. Frequencies and relative intensities for the identified lines are listed in Table 2.

**Rotational Structure.** Before we can perform a vibrational analysis of the spectrum, we must consider the possibility that some of the observed structures actually represent partially resolved rotational structures. Recently, we have extended the rigid rotor model for the description of a van der Waals complex (developed for example in refs 50 and 51) to the case of two-photon absorption.<sup>41</sup> Two-photon absorption processes are characterized by either a zeroth rank tensor or the components of a second rank tensor or both. For the calculation of the two-photon transition probabilities, it is assumed that the excitation is confined to the acetaldehyde molecule within the complex. The relevant components of the two-photon absorption operator for the complex are calculated by transforming the correspond-

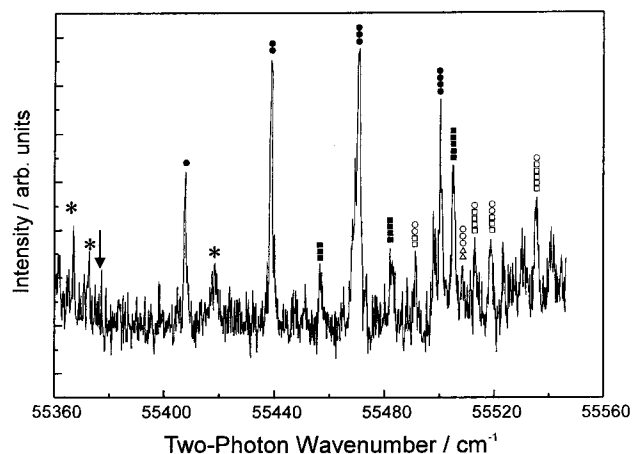


**Figure 5.** Expanded (2 + 1) REMPI spectrum of the acetaldehyde–Ar complex correlating with the monomer band 10<sup>1</sup><sub>0</sub>. The arrow indicates the possible position of the origin for this band system. Vibrational bands are marked with the number of vibrational quanta involved. The features marked with an asterisk are artifacts due to a baseline shift caused by strong monomer signals at these frequencies. See text for details.

**TABLE 2: Two-Photon Wavenumbers  $\nu$  and Relative Franck–Condon Factors  $x_{fc}$  of the Observed Vibronic Bands of the Acetaldehyde–Ar Complex in an Electronic State Correlating With the 10<sup>1</sup><sub>0</sub> Level of the (n,3s) Rydberg State**

mode	$\nu_c, \nu_s, \nu_t$	$\nu$ (cm <sup>-1</sup> )	$\Delta\nu$ (cm <sup>-1</sup> ) <sup>a</sup>	$x_{fc}$
square	0,3,0	55456.6	25.5	7.5
	0,4,0	55482.1	22.8	7.5
	0,5,0	55504.9		20.0
circle	0,0,0	55376.2		<0.5
	1,0,0	55407.7	31.5	22.0
	2,0,0	55438.7	32.2	48.0
	3,0,0	55470.9	29.6	63.0
	4,0,0	55500.5		32.5
	3,0,2	55508.6		10.0
	1,4,0	55513.1	22.7	14.5
	1,5,0	55535.8		13.0
	2,2,0	55491.4	27.5	13.5
	2,3,0	55518.9		15.5

<sup>a</sup> Frequency intervals  $\Delta\nu$  between different members of the assigned progressions.

ing tensor components for the two-photon chromophore to the principal axis system of the complex. In the case of a nonvanishing second rank tensor component, all five components will in general contribute to the spectrum of the complex. For acetaldehyde, we have shown that the two-photon transition is dominated by a zeroth rank tensor component which transforms like a scalar.<sup>14</sup> The rotational structure is therefore dominated by Q-branches. Since the rotational constants for the excited Rydberg state are similar to the ones in the electronic ground state, the rotational structure of the Q-branches cannot be resolved with the present resolution. This also implies that the two-photon spectra of the complex will be dominated by unresolved Q branches. Furthermore, at the achieved temperatures in our molecular beam expansion, we do not expect hot bands of intermolecular modes to contribute to the spectrum. Along the same line of reasoning, we exclude the possibility of population of excited levels involving the methyl torsion. Therefore, the spectra reported here represent exclusively the vibrational structure of the complex in its excited electronic state.

**Vibrational Structure.** As an atom–molecule system, we expect three intermolecular vibrations for the acetaldehyde–Ar complex, one stretching and two bending modes. As a first



approximation, at least the low-frequency part of the spectrum should be analyzable in terms of three harmonic frequencies. The vibrational structure of the spectrum is clearly dominated by a progression (labeled with solid circles in Figure 4) with at least four members. All members are separated by about  $32\text{ cm}^{-1}$ , which we denote as the mode  $\nu_c$ . It is interesting to note that no anharmonicity is observed for this progression. As a van der Waals complex with possible large-amplitude motion, we do not expect the modes to be independent and harmonic. On the other hand, given the complicated vibrational structure observed experimentally, we try to exploit the fact that the observed lines for at least one mode are consistent with the harmonic approximation. Therefore, we try to identify line separations corresponding to one or more quanta in  $\nu_c$  by assuming that possible combination bands will show only small anharmonicities in the latter vibration. With this assumption made, all lines except the ones marked in Figure 4 with solid squares or triangles can be understood involving at least one quantum of the  $\nu_c$  vibration. Within the set of unaccounted lines, we identify easily a second progression labeled with solid squares in Figure 4. The spacings indicate a slightly smaller harmonic frequency of about  $\nu_s = 27\text{ cm}^{-1}$ . We also identify progressions in  $\nu_s$  which involve one and two quanta of  $\nu_c$  marked with open symbols. The assignments in terms of the three modes  $\nu_c$ ,  $\nu_s$ , and  $\nu_t$  are included in Table 1. Most noticeable is the absence of any anharmonicity for the progressions involving the mode  $\nu_c$ . In contrast, all progressions in the mode  $\nu_s$  show small anharmonicities although the trend is not as clear as in the case of a one-dimensional oscillator.

At the low-frequency end of the spectrum, another weak band marked with two solid triangles is found. This band is shifted by  $10\text{ cm}^{-1}$  to the blue of the first observed member of the progression in the mode  $\nu_c$  and its harmonic frequency is denoted  $\nu_t$ . Built on this band, we find another progression with the characteristic spacing of  $32\text{ cm}^{-1}$ , i.e., combination bands involving an increasing number of quanta  $\nu_c$ .

The progressions in the modes  $\nu_s$  and  $\nu_c$  show intensity distributions compatible only with significant changes in the equilibrium structure for the excited state potential energy surface of the complex. Therefore, the exact location of the origin for this band system is not necessarily given by the position of the first observed member. To explore different possibilities for the location of the origin, we recognize that the strong progression in the mode  $\nu_c$  does not show any anharmonicity. Using the constant interval of about  $32\text{ cm}^{-1}$ , we identify as another possible location of the origin a frequency of  $55\,038.6\text{ cm}^{-1}$ . This position of the origin, marked with an arrow in Figures 3 and 4, falls into a region where baseline shifts due to strong monomer signals cannot be avoided. As can be seen in Figure 3, the peak to the left of the arrow coincides clearly with the weak rotational structure observed for the monomer at this frequency. With the present signal-to-noise ratio, it was not possible to detect an unambiguous signal due to the complex in this frequency range.

On the other hand, a very weak band is observed at  $55\,061\text{ cm}^{-1}$ , i.e., to the red of the first observed member of the progression in  $\nu_c$ . At the low temperatures in the molecular beam, the population of excited intermolecular vibrational levels is very unlikely. Furthermore, the other members of this progression do not show a satellite red shifted by the same amount. Consequently, we must assign this band to an intermolecular vibration of the excited state. This assignment is supported by the fact that the weak band marked with two triangles in Figure 4 is located at the position roughly expected

for the first overtone. A shift in the origin of the band system results in an increase of the quantum numbers  $\nu_c$  and  $\nu_t$  by 1. For the progression in  $\nu_s$ , we expect the first member to be located on the red side of the first member of the progression in  $\nu_c$ . A careful inspection indeed reveals a very weak band located in the red tail of this band. The close values for the harmonic frequency of the modes  $\nu_s$  and  $\nu_c$  result in pairs of combination bands which differ in one quantum of each vibration. For example, two closely spaced lines are found at  $55\,130$ ,  $55\,156$ , and  $55\,192\text{ cm}^{-1}$ . As a result of this analysis, we find the three harmonic frequencies  $\nu_c = 32\text{ cm}^{-1}$ ,  $\nu_s = 27\text{ cm}^{-1}$ , and  $\nu_t = 21\text{ cm}^{-1}$  for the three intermolecular modes. Only the high-frequency modes are Franck–Condon active.

As can be seen in Figure 5, the band system to the blue of the monomer band  $10^1_0$  is also dominated by a progression in the mode  $\nu_c$ . The bands show a spacing and intensity distribution very similar to the system correlating with the origin band of the monomer. Following the same line of reasoning as before, we assume that the first observed band represents actually the second member of this progression. This yields a frequency of  $55\,376.2\text{ cm}^{-1}$  for the origin of this band system corresponding to a blue shift of  $18.0\text{ cm}^{-1}$ . Although the signal-to-noise ratio is very poor, we can identify additional combination bands involving the mode  $\nu_c$  and several members of the progression in the vibration  $\nu_s$ . The assignments are included in Table 2.

While the assignments given so far are consistent with the line positions as well as the intensity distributions in the various progressions, the assignments, especially for levels with higher energy, must be considered tentative. Strong anharmonicities close to the dissociation limit cannot allow an unambiguous assignment. Furthermore, the coupling of different vibrational modes, in particular for levels with very similar energies, must result in further ambiguities.

#### 4. Discussion

Several features about the recorded spectra are quite surprising and warrant further discussion. (1) The detected band systems exhibit small blue shifts with respect to the corresponding vibronic monomer bands, thus indicating a very similar, but lower binding energy in the excited state. (2) The main band system displays a threshold-like behavior, although, above this threshold, the signal does not disappear completely. (3) Two modes are Franck–Condon active giving rise to long progressions. The progressions show only very small anharmonicities.

Considering the Rydberg nature of the excited state, we would expect a red-shifted rather than a blue-shifted spectrum for the complex. Usually, ion-induced dipole interaction results in a strong ionic character for the bonding in the excited Rydberg state. The increased well depth of the excited state potential should give rise to a red shift of the spectrum. Therefore, we considered initially the alternative interpretation that the observed strong cluster spectrum is built upon the  $10^1_0$  mode, thus indicating a considerable red shift of the spectrum. Since the monomer  $0^0_0$  band is much stronger than the band  $10^1_0$ , we searched without success for an intense cluster feature to the red of the monomer origin. Although this negative result seems to confirm the blue shift of the complex band with respect to the origin band, one must consider the restricted applicability of the (2 + 1) REMPI detection scheme employed in these experiments. With an ionization potential of  $82\,526.5\text{ cm}^{-1}$ , (2 + 1) REMPI spectroscopy of the acetaldehyde monomer is limited to states which lie at least  $55\,018\text{ cm}^{-1}$  above the ground state.<sup>52</sup> Thus, the origin of the Rydberg state for the monomer lies only  $6\text{ cm}^{-1}$  above this threshold. For lower lying

intermediate states, two photons are required for the ionization step, reducing the efficiency of the REMPI process dramatically. Therefore, cluster bands which exhibit only a small red shift might not be accessible through an efficient (2 + 1) REMPI detection scheme. To avoid these difficulties, we searched for such red-shifted bands employing a two-color (2 + 1') REMPI scheme. Nevertheless, even this scheme did not result in the detection of a cluster signal to the red of the origin band. Subsequent careful searches to the blue of the  $10^1_0$  mode revealed the extremely weak cluster band with a vibrational structure almost identical to the one found for the stronger cluster band.

The argument for the expected red shift of the cluster band is based on the assumption of a stronger bond in the excited state due to the ion-induced dipole interaction. The cationic character of the complex would be especially pronounced if the radius of the excited electron orbital is on the average larger than the van der Waals radius of the argon atom. Therefore, the argon atom can be regarded as a sensitive probe of the electron density in the excited state. On the other hand, the situation would be more complicated if the radius is smaller or similar to the van der Waals radius of the complexed atom. To determine an estimate for the radius of the electron in the excited 3s orbital, we determine the effective principal quantum number  $n^*$  from the relative position of the excited energy level with respect to the ionization limit IP, using the notation<sup>53</sup>

$$n^* = \sqrt{\frac{R_\infty}{\text{IP} - h\nu_{00}}}, \quad R_\infty = \text{Rydberg constant}$$

From this expression, we find an effective principal quantum number  $n^* = 2.0$  for the (n,3s) Rydberg state. Accordingly, the radius  $r$  of the electron orbital is estimated to be  $r = a_0 n^{*2} = 2 \text{ \AA}$  which is considerably smaller than the van der Waals radius of the argon atom. Since the electron in the excited Rydberg state is mostly confined to an orbital located between the argon atom and the cationic core of the acetaldehyde molecule, it is reasonable that the positive charge of the core is well shielded, resulting in a weakening of the van der Waals bond in the excited state.

The vibrational analysis of the observed bands yields 55 038.6  $\text{cm}^{-1}$  as the location of the electronic origin. Thus, the origin of the band system is blue shifted by about 14.1  $\text{cm}^{-1}$  from the corresponding origin of the monomer. Similarly, the band built upon the  $10^1_0$  mode is shifted to the blue by 18.0  $\text{cm}^{-1}$ , indicating an additional weakening of the van der Waals bond.

These observed trends can be rationalized in terms of structural changes occurring upon excitation to the Rydberg state. For the ground state, Ioannou et al. determined a nonplanar structure with the Ar atom sitting on top of the CCO triangle.<sup>44</sup> Therefore, it is not too surprising that excitation of the CCO bending vibration influences the spectrum of the complex. In their calculation of the acetaldehyde monomer, Wiberg et al. find for the excited state a considerable enhancement of the polarization of the carbonyl group and an increased negative charge on the methyl carbon atom.<sup>54</sup> The changes in the electron density are responsible for a decreased C–O bond distance and an increased C–C–O bond angle. These trends are consistent with the experimentally determined change in the A rotational constant found for this Rydberg state.<sup>14</sup> For the complex, the shift in electron density could produce an increased short-range repulsion, causing an increase in the height of the in-plane barrier to internal rotation. As a consequence, the argon atom is forced further out of the plane, causing the destabilization of

the complex and the observed blue shift of the spectrum. Excitation of the C–C–O bending vibration further increases the C–C–O angle causing the small additional blue shift of the band system correlating with the monomer band  $10^1_0$ .

The intensity drop at a frequency of about 55 240  $\text{cm}^{-1}$  can be understood in terms of at least three different scenarios. (1) At an energy of about 200  $\text{cm}^{-1}$  above the origin, the barrier to internal rotation of the acetaldehyde unit within the complex is surpassed making different rovibrational levels above the barrier accessible. (2) Alternatively, this energy almost coincides with the energy of the first excited level of the methyl torsion in the Rydberg state. (3) Finally, the intensity drop can be indicative of the dissociation limit of the complex itself.

As pointed out by Ioannou et al. in ref 44, one of the two possible tunneling pathways can be visualized as a motion of the Ar atom from one side of the acetaldehyde molecule to the other. In this case, the actual tunneling motion is most likely restricted to the internal rotation of the acetaldehyde unit within the complex. The axis of internal rotation is thus close to the a-inertial axis of acetaldehyde. To explore the possibility of internal rotation of the acetaldehyde unit, we calculated energy levels for a one-dimensional model system assuming a symmetric double well potential. Within this model, we tried to find a correlation between the rotational constant  $F$  of the internal rotor (assuming a rigid acetaldehyde unit) and the energy level spacing for a given barrier of about 200  $\text{cm}^{-1}$ . The observed energy level spacing of about 30  $\text{cm}^{-1}$  can be reproduced with an  $F$  constant of 1.3  $\text{cm}^{-1}$ , which is comparable in magnitude to the A rotational constant of the acetaldehyde monomer ( $A' = 1.99 \text{ cm}^{-1}$ ). The calculated levels show a noticeable splitting into two parity levels, especially near the barrier. Approaching the barrier, the position of the energy levels is characterized by a much stronger anharmonicity than observed experimentally.

Another possible explanation for the feature observed in the experiment is activation of the methyl torsion upon complexation. In the monomer, transitions with  $\Delta v_{15} \neq 0$  are extremely weak because of poor Franck–Condon factors. These transitions are reduced in intensity by at least several orders of magnitude in comparison with the intensity of the torsional sequence bands ( $\Delta v_{15} = 0$ ). If the transition involves an odd number of quanta in the torsional mode, only transitions between levels of the symmetry species E are allowed. For the monomer, these “forbidden” transitions show a clear propensity for  $\Delta v_{15} = \text{even}$ , which we expect to hold true also for the complex. On the other hand, structural changes occurring upon complexation might result in a substantial increase of the overlap integrals. For this reason, we would expect a transition with  $\Delta v_{15} = 2$  to be significantly stronger than the excitation of the first excited torsional level. As can be seen in Figure 3, this torsional band corresponding to the excitation of the first overtone is expected near 55 400  $\text{cm}^{-1}$ . In this wavelength range, we find only the weak cluster band system with a vibrational structure very similar to the one found for the system near the origin band. The frequency shift of this system is comparable to the one built upon the origin band. Therefore, we assign this system to the  $10^1_0$  mode in the acetaldehyde–Ar complex rather than the excitation of the methyl torsion.

Finally, the observed threshold behavior can be interpreted as the dissociation limit of the complex in its excited state. Assuming a Lennard–Jones potential, Ioannou et al. derived an estimate of 204  $\text{cm}^{-1}$  for the binding energy of the ground state.<sup>44</sup> Combining these results with the observed blue shift of 14  $\text{cm}^{-1}$ , we find an excited-state dissociation energy of 190

$\text{cm}^{-1}$ . The dissociation limit for the complex is thus reached at a laser frequency of about  $55\,230\text{ cm}^{-1}$ . This value coincides extremely well with the frequency at which the vibrational structure disappears and the intensity suddenly drops. The last clearly resolved vibrational band is found at a frequency of  $55\,206\text{ cm}^{-1}$ .

Nevertheless, even at frequencies higher than the threshold, weak unstructured signals due to unfragmented complexes are detected. This behavior is consistent with the assumption that at least one of the Franck–Condon active modes,  $\nu_c$  or  $\nu_s$ , is only weakly coupled to the dissociation coordinate. A weak coupling to the stretching coordinate would allow for long lifetimes of excited vibrational levels involving a bending mode even if the total energy exceeds the dissociation limit. As long as the ionic state reached in the ionization process is sufficiently stable, efficient REMPI detection of the complex is feasible even if the lifetime of the Rydberg state is only a fraction of the laser pulse duration (about 5 ns in our experiment).

Both active intermolecular modes exhibit almost no anharmonicity even at energies as high as 60% of the dissociation energy. In light of the small change in the dissociation energy, it is thus very likely that these active modes represent mainly motion along the two intermolecular bending coordinates. The lack of anharmonicity implies further that the barriers to internal rotation must be considerably higher than the dissociation energy of the complex. Since we observe long progressions in these modes, the new equilibrium position of the acetaldehyde unit must be rotated away from its ground-state position. On the other hand, the absence of a strong progression in the third mode  $\nu_t$ , most likely involving motion along the dissociation coordinate, implies that only small changes in the radial distance occur upon excitation to the Rydberg state. Following this line of reasoning, we conclude that the new minimum configuration of the complex corresponds to a rotation rather than a combination of translation and rotation. The observed small frequency shift indicates further that the rotated equilibrium position is characterized by a value for the dissociation energy very similar to the one found for the electronic ground state.

## 5. Conclusions

In this contribution, we have shown that it is possible to detect efficiently van der Waals complexes involving polyatomic molecules through a (2 + 1) REMPI process. The observed band systems of the acetaldehyde–Ar complex correlate with the monomer bands  $0^0_0$  and  $10^1_0$  for excitation to the (n,3s) Rydberg state. Both bands are blue shifted from the corresponding monomer bands, indicating a small effective size of the Rydberg orbital and an increased in-plane barrier to internal rotation of the acetaldehyde unit. The resulting shift in the position of the Ar atom explains the dominant progressions in the intermolecular bending vibrations and the absence of a noticeable anharmonicity. At least one of the bending modes is only weakly coupled to the stretch vibration, allowing the excitation of bending levels near the dissociation limit. An estimate of  $190\text{ cm}^{-1}$  for the latter is derived from the observed disappearance of the vibrational structure. In combination with the blue shift of the spectra, the dissociation limit is in excellent agreement with the data derived for the ground state by Ioannou et al.<sup>44</sup>

**Acknowledgment.** Financial support from the National Science Foundation is gratefully acknowledged. We also thank

the reviewers for carefully reading the manuscript and for many helpful suggestions.

## References and Notes

- (1) Bacic, Z.; Miller, R. E. *J. Phys. Chem.* **1996**, *100*, 12945.
- (2) See, for example: *Faraday Discuss.* **1994**, *97*.
- (3) Seelemann, T.; Andresen, P.; Schleipen, J.; Beyer, B.; ter Meulen, J. J. *J. Chem. Phys.* **1988**, *126*, 27.
- (4) Meyer, H. *J. Chem. Phys.* **1994**, *101*, 6686.
- (5) Meyer, H. *J. Chem. Phys.* **1994**, *101*, 6697.
- (6) Meyer, H. *J. Chem. Phys.* **1995**, *102*, 3151.
- (7) Sanov, A.; Droz-Georget, Th.; Zyrianov, M.; Reisler, H. *J. Chem. Phys.* **1997**, *106*, 7013.
- (8) Sitz, G. O.; Kummel, A. C.; Zare, R. N. **1988**, *89*, 2558.
- (9) Rakitzis, T. P.; Kandel, S. A.; Lev-On, T.; Zare R. N. *J. Chem. Phys.* **1997**, *107*, 9392.
- (10) Heath, B. A.; Robin, M. B.; Kuebler, N. A.; Fisanik, G. J.; Eichelberger, T. S. *J. Chem. Phys.* **1980**, *72*, 5565.
- (11) Gu, H.; Kundu, T.; Goodman, L. *J. Phys. Chem.* **1993**, *97*, 7194.
- (12) Buntine, M. A.; Metha, G. F.; McGilveray, D. C.; Morrison, R. J. S. *J. Mol. Spectrosc.* **1994**, *165*, 12.
- (13) Shand, N. C.; Ning, C. L.; Pfab, J. *J. Chem. Phys. Lett.* **1995**, *247*, 32.
- (14) Meyer, H. *J. Chem. Phys. Lett.* **1996**, *262*, 603.
- (15) Kim, Y.; Fleniken, J.; Meyer, H. *J. Chem. Phys.* **1998**, *109*, 3401.
- (16) Barker, J. R., Ed. *Progress and problems in atmospheric chemistry; Advanced series in physical chemistry*; World Scientific: Singapore, 1995; Vol. 3.
- (17) Parmenter, C. S. *J. Phys. Chem.* **1982**, *86*, 1735.
- (18) Moss, D. B.; Parmenter, C. S. *J. Chem. Phys.* **1993**, *98*, 6897.
- (19) Timbers, P. J.; Parmenter, C. S.; Moss, D. B. *J. Chem. Phys.* **1994**, *100*, 1028.
- (20) Moss, D. B.; Parmenter, C. S.; Ewing G. E. *J. Chem. Phys.* **1987**, *86*, 51.
- (21) Spangler, L. H.; Pratt, D. W. *J. Chem. Phys.* **1986**, *84*, 4789.
- (22) Richard, E. C.; Walker, R. A.; Weisshaar, J. C. *J. Chem. Phys.* **1996**, *104*, 4451.
- (23) Tan, X. Q.; Majewski, W. A.; Plusquellic, D. F.; Pratt, D. W. *J. Chem. Phys.* **1991**, *94*, 7721.
- (24) Kim, Y.; Fleniken, J.; Meyer, H. Work in progress.
- (25) Nesbitt, J. *Annu. Rev. Phys. Chem.* **1994**, *45*, 367.
- (26) Miller, R. E. In *Advances in Molecular Vibrations and Collision Dynamics*; Bowman, J. M., Bacic, Z., Eds.; JAI Press: New York, 1991; Vol. IA.
- (27) Heaven, M. C.; Chen, Y.; Lawrence, W. G. In *Advances in Molecular Vibrations and Collision Dynamics*; Bowman, J. M., Bacic, Z., Eds.; JAI Press: New York, 1998; Vol. III.
- (28) Schwartz, R. L.; Giancarlo, L. C.; Loomis, R. A.; Bonn, R. T.; Lester, M. I. *J. Chem. Phys.* **1996**, *105*, 10224.
- (29) Djafari, S.; Barth, H.-D.; Buchhold, K.; Brutschy, B. *J. Chem. Phys.* **1997**, *107*, 10573.
- (30) Matsumoto, Y.; Ebata, T.; Mikami, N. *J. Chem. Phys.* **1998**, *109*, 6303.
- (31) Pribble, R. N.; Zwier, T. S. *Science* **1994**, *265*, 75.
- (32) Milce, A. P.; Heard, D. E.; Miller, R. E.; Orr, B. J. *J. Chem. Phys. Lett.* **1996**, *250*, 95.
- (33) Schaefer, M. W.; Maxton, P. M.; Felker, P. M. *Chem. Rev.* **1994**, *94*, 1787.
- (34) Rudich, Y.; Naaman, R. *J. Chem. Phys.* **1992**, *96*, 8618.
- (35) Ni, H.; Serafin, J. M.; Valentini, J. J. *J. Chem. Phys.* **1996**, *104*, 2259.
- (36) Miller, J. C.; Cheng, W. C. *J. Phys. Chem.* **1985**, *89*, 1647.
- (37) Suzuki, T.; Katayanagi, H.; Heaven, M. C. *J. Phys. Chem.* **1997**, *101*, 6697.
- (38) Green, D. S.; Wallace, S. C. *J. Chem. Phys.* **1994**, *100*, 6129.
- (39) Koekhoven, S. M.; Buma, W. J.; de Lange, C. A. *J. Chem. Phys.* **1995**, *102*, 4020.
- (40) Meyer, H. *J. Chem. Phys.* **1997**, *107*, 7721.
- (41) Meyer, H. *J. Chem. Phys.* **1997**, *107*, 7732.
- (42) Mack, P.; Dyke, J. M.; Smith, D. M.; Wright, T. G.; Meyer, H. *J. Chem. Phys.* **1998**, *109*, 4361.
- (43) Fleniken, J.; Kim, Y.; Meyer, H. *J. Chem. Phys.* **1998**, *109*, 8940.
- (44) Ioannou, I. I.; Kuczkowski, R. L. *J. Mol. Spectrosc.* **1994**, *166*, 354.
- (45) Ioannou, I. I.; Kuczkowski, R. L.; Hougén J. T. *J. Mol. Spectrosc.* **1995**, *171*, 265.
- (46) Wright, S. A.; Dagdigian, P. J. *J. Chem. Phys.* **1997**, *107*, 680.

- (47) Van de Burgt, L. J.; Heaven, M. C. *J. Chem. Phys.* **1988**, *89*, 2768.  
(48) Crighton, J. S.; Bell, S. *J. Mol. Spectrosc.* **1985**, *112*, 304.  
(49) Noble, M.; Lee K. C. *J. Chem. Phys.* **1984**, *81*, 1632.  
(50) Mills, P. D. A.; Western, C. M.; Howard, B. J. *J. Phys. Chem.* **1986**, *90*, 3331.  
(51) Fawzy, W. M.; Hougen, J. T. *J. Mol. Spectrosc.* **1989**, *137*, 154.  
(52) Brint, P.; O'Toole, L.; Mayhew, C. A.; Dussa, W. *J. Chem. Soc., Faraday Trans.* **1990**, *86*, 3349.  
(53) Lefebvre, H.; Field, R. W. *Perturbations in the spectra of diatomic molecules*; Academic: New York, 1986.  
(54) Hadad, C. M.; Foresman, J. B.; Wiberg, K. B. *J. Phys. Chem.* **1993**, *97*, 4293.